

## Three dimensional visualization and comparison of impressions on fired bullets

Atsuhiko Banno<sup>a,b,\*</sup>, Tomohito Masuda<sup>a</sup>, Katsushi Ikeuchi<sup>a</sup>

<sup>a</sup>*Ikeuchi Laboratory 4-6-1, Institute of Industrial Science, University of Tokyo, Komaba, Meguro-ku, Tokyo 153-8505, Japan*

<sup>b</sup>*National Research Institute of Police Science 6-3-1, Kashiwanoha, Kashiwa, Chiba 227-0882, Japan*

Received 1 September 2003; received in revised form 15 November 2003; accepted 18 November 2003

### Abstract

Currently, optical devices, such as microscopes and CCD cameras, are utilized for identification of bullets and tool marks in the field of forensic science. While these optical methods are easily manageable and effective, they are under great influence of illumination condition. In other words, appearances of striations through these optical devices have possibility to be changed by lighting condition. Besides these appearance-based approaches, we can utilize three dimensional (3D) geometric data of tool marks that are free from lighting condition. In this study, we focused on 3D geometric data of landmark impressions on fired bullets for identification. We obtained the 3D surface data of tool marks by a confocal microscope and reconstructed virtual impressions on a PC monitor from the geometric data. Furthermore, the 3D data are exploited to numerical matching of two surface shapes. We also visualized the difference of two shapes. In order to do this, two surface models are aligned automatically. In this process, pairings of correspondent points on both surfaces are determined. Distance analysis between these pairs leads to a shape comparison. Since comparison results are visualized, they are intuitive and easily perceptive.

© 2003 Published by Elsevier Ireland Ltd.

**Keywords:** Three dimensional; Fired bullets; Alignment; Shape difference

### 1. Introduction

A lot of striation and impression marks caused by various ordinary tools, such as a screw driver, a crowbar and a hammer, are left at crime scenes. These marks are significant evidences. Especially, striation marks on a fired bullet are important for identifying the suspicious firearm. Forensic scientists identify these striations mainly by using optical tools such as comparison microscopes, CCD cameras, and photos. The surfaces of striation have three dimensional (3D) roughness intrinsically. By using optical devices, we compare reflectance images instead of 3D shapes. These appearance-based methods are effective and easily manageable. Appearances of striations through these devices, however, depend on location of light and viewpoint. In other

words, same striation has possibility to look different under different lighting condition.

Besides these appearance-based methods, we are also able to exploit 3D geometric data of striations. That is model-based methods. The measurement of small elevations on a striation had been difficult in aspect of hardware. However many sophisticated 3D measurement devices are developed recently and we can easily obtain fine 3D maps of striation surfaces. The shape of striation surface is expected to be printed intrinsic shapes of the tool that caused the striation marks. Moreover, 3D data are independent of lighting condition.

Although there are some researches on 3D surfaces of bullets and tool marks [1–3], they had not led to shape comparisons by using 3D surface data directly. In the field of Japanese archaeology, Masuda et al. [4] have analyzed shape difference of ancient bronze mirrors with a method of computer vision. In this study, we apply this method to identification of bullets. We focused on the surface shapes of fired bullets, especially landmark impressions, and

\* Corresponding author. Tel.: +81-3-5452-6242;  
fax: +81-3-5452-6244.  
E-mail address: [vanno@cvi.iis.u-tokyo.ac.jp](mailto:vanno@cvi.iis.u-tokyo.ac.jp) (A. Banno).

visualized the shapes in a PC monitor. In addition, we compared these 3D shapes numerically. The distance of two surfaces is calculated for the evaluation of shape matching. Visualizing the distance, we are able to recognize the difference of two shapes at a glance.

## 2. Visualization of surfaces

### 2.1. Acquisition of 3D data

We obtained 3D data of striations surfaces by a confocal microscope based on an optical principle. The device measures values of observed intensity at all measuring points (pixels) while moving the stage vertically. The confocal optics has a characteristic that the stage position with maximal intensity coincides the position on focus at a point on the surface (Fig. 1). Therefore, by memorizing each stage where the point has the maximal intensity, the device is able to reconstruct the surface topography. We use a confocal microscope (HD100D-A, Lasertec Co. Ltd.), which can measure  $3.2 \text{ mm} \times 3.2 \text{ mm}$  region with  $450 \times 450$  pixels with  $0.02 \mu\text{m}$  resolution in term of height. The measurement results are represented as gray scale images called range images (Fig. 2), where height of elevation is converted into a gray scale value at each point. This map indicates whiter pixel indicates more elevated point. To reduce the influence of noise and outlier, a Gaussian filter and a median filter are applied to the range images. Then we can obtain the  $(x, y, z)$ -values of all pixels on a range image by multiplying magnifications.

### 2.2. Visualization

Next, we visualize the surface topographies on a PC monitor. Visualization leads us to perceive the surface topography intuitively.

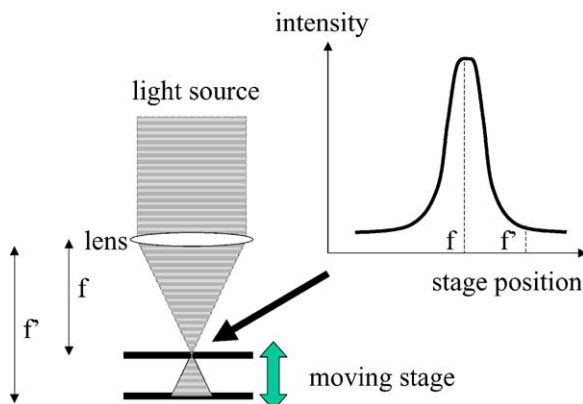


Fig. 1. The principle of a confocal optics. This system has characteristics that intensity of a measuring point is maximal when the point is on focus. By moving the stage, the device memorizes each stage position of maximum intensity at each pixel. A collection of each stage position can reconstruct the surface model.



Fig. 2. A range image ( $450 \times 450$  pixels). In this image, gray scale indicates elevation of the surface. The whiter the pixel, the nearer the position.

Visualization procedure is followed. First, a measured surface is represented as a set of triangle patches. A shape and color (shading) of each triangle are calculated by using the normal vector of the triangle, a direction of a light source and a position of viewpoint. Then a whole appearance of a virtual landmark impression, which is a collection of numerous these triangle patches, is displayed on a PC monitor. Moreover, a direction of light source and a position of viewpoint are easily changeable by dragging a mouse. In other words, we can observe a virtual impression from arbitral viewpoint under arbitral lighting condition.

Let us explain more detail about shading. As mentioned above we can regard a surface consists of numerous triangle patches. Then we will consider one of these patches. For visualization, we must consider three important directions; the direction of the light source, the normal direction of the patch, and the viewpoint direction (Fig. 3). The color and the brightness of an object surface depend on the relationship of these three directions. Several models to describe this relationship have been proposed in the field of computer graphics. In this study, we adopt the Phong's model, which simulates three components, which are ambient, diffuse, and specular reflection.

$$C = C_{\text{Ambient}} + C_{\text{Diffuse}} \cos \alpha + C_{\text{Specular}} \cos^n \beta$$

$$\cos \alpha = \mathbf{L} \cdot \mathbf{N}, \quad \cos \beta = 2(\mathbf{L} \cdot \mathbf{N})(\mathbf{N} \cdot \mathbf{V}) - \mathbf{L} \cdot \mathbf{V}$$

where  $\mathbf{L}$  is the direction of light source,  $\mathbf{N}$  is the normal vector,  $\mathbf{V}$  is the direction of viewpoint.

Shading of each triangle patch is calculated the above formulation. A PC renders all merged patches and we can observe virtual objects on the monitor.

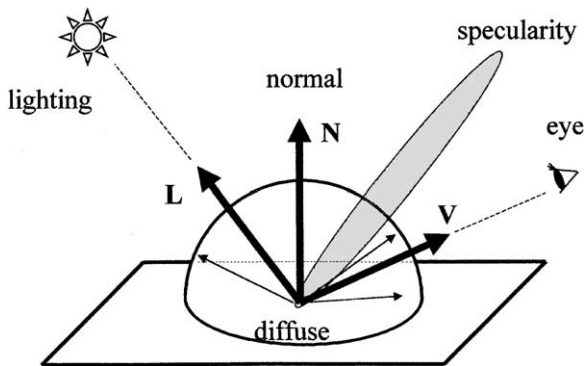


Fig. 3. A physical reflection model. Brightness of surface element depends on three vectors: Specularity means highlight, which we perceive a strong reflection of light source. The direction of specularity, however, is limited in so narrow that we perceive brightness of the surface element equal to diffuse component except from this direction.

We use OpenGL as a graphic library so that a PC can display a virtual landmark impression quickly and comfortably. Furthermore, dragging a mouse changes the location of a viewpoint and light sources easily and quickly.

### 3. Comparison of surfaces

#### 3.1. Alignment of 3D data

Generally speaking, it is impossible to locate a real bullet on the stage of a microscope in the identical position at each measurement. Therefore, each representation co-ordinate system of a measurement differs from that of other measurements. To compare two shapes, we must move their co-ordinates in order to coincide two surfaces better. If the two striations are derived from the same origin, the shapes will be similar. Furthermore, if we could calculate the distance of the two shapes' difference, similarity of two shapes would be estimated according to the distance.

We adopted the alignment method [5], which is a kind of ICP method [6] for shape matching.

To simplify the moving procedure, we assume that one shape is fixed and another can move. We call the fixed shape "model shape" and the movable one "data shape". Rotating and translating data shape align two shapes. If two shapes are same, a point on the model shape has the corresponding point on the data shape. Which is the corresponding point, however, is usually unknown. Then, we resolve this correspondence problem by iterative method. Initially a temporal corresponding point is assumed. A movement is determined so as to minimize an objective function, which is defined by distances between the corresponding points. The temporal correspondences are changed after the movement. Then a new movement is

determined under the new temporal correspondence, again. This procedure is repeated until the total distance converges. The objective function, which should be minimized for the alignment, is defined as:

$$f(\mathbf{R}, \mathbf{t}) = \sum_{i,j} [\mathbf{R}x_i + \mathbf{t} - y_{ji}]$$

where  $\mathbf{R}$  is the rotation matrix,  $\mathbf{t}$  is the translation vector,  $x_i$  is the  $i$ th point in seine data,  $y_{ji}$  is the corresponding point in the  $j$ th is the model data for  $x_i$ .

This objective function indicates the summation of distances between all pairs of corresponding points. Initially the function takes high values because there are a lot of wrong relationships of correspondences. As iterating calculations, wrong correspondences are improved and the function takes a converged value. If two shapes coincide, the function takes a low value. When the function converges under a threshold, we decide two shapes are similar.

We use quaternion to minimize the objective function. By substituting quaternion  $\mathbf{q}$  to rotate matrix  $\mathbf{R}$ , motion vector  $\mathbf{p}$  can be found as follows:

$$\mathbf{p} = \operatorname{argmin}_{\mathbf{R}, \mathbf{t}} f(\mathbf{R}, \mathbf{t}) = \operatorname{argmin}_{\mathbf{q}, \mathbf{t}} f(\mathbf{q}, \mathbf{t})$$

$$\text{where } \mathbf{q} = [u \ v \ w \ s]$$

Motion vector  $\mathbf{p}$ , that is  $\mathbf{q}$  and  $\mathbf{t}$ , is solved by the conjugate gradient method and line minimization with golden section search [5]. The solutions are the ones that minimize the objective function.

#### 3.2. Shape difference

Above alignment determines the relationship of corresponding points. Therefore, the distance between each pair of corresponding points can be calculated (Fig. 4). We regard these distances of the corresponding points will be a cue of shape matching. If the distance of a pair is less than a threshold, the correspondence is regarded as right.

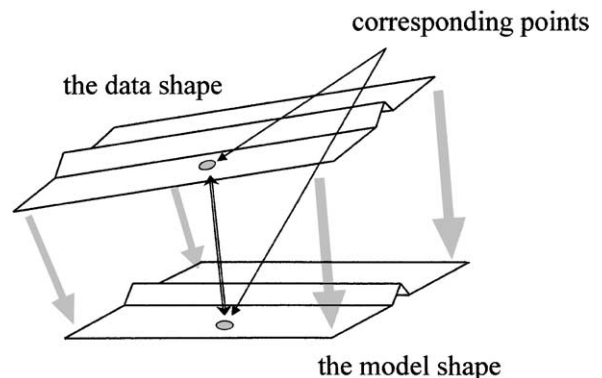


Fig. 4. A concept of the distance of two shapes. The distance is defined as the summation of distances between corresponding points. In order to minimize the distance, the data shape is moved while the model shape is fixed.

Otherwise, the pair do not have correspondence; namely two shapes do not match at this part.

In terms of shape matching of two surfaces, wide region of non-matching indicates that two shapes are different.

By the way, all programs used in this study are produced in our laboratory by using Microsoft Visual C++, version 6.0.

## 4. Experiments

### 4.1. Visualization

At first we used two 0.25 in. caliber bullets fired from the same firearm (a Tanfoglio auto model GT27). Each bullet has six landmark impressions with about 1.7 mm width.

This measurement device (the confocal microscope) is equipped with a calibrated stage, which enables to merge precisely several adjacent surface dataset. In this experiment, we connected four rectangular regions ( $4 \times 4$ ). As mentioned above, a range image file has  $450 \times 450$  pixels and each pixel has 16-bit signal, that is 65,536 resolution in terms of elevation. Therefore, 3D data are very compact (a range data file needs only 405 kB memory as a RAW file).

A perspective view of a landmark impression and a reflectance image of the same impression are shown in Fig. 5. While left view of the reflectance image is very

vivid, it is difficult to comprehend 3D surface topography. On the other hand, 3D perspective image are very intuitive and makes us perceive the roughness on the surface.

In some reflectance images, a shallow stria happens to look like a deep one. This indicates that a trivial stria has possibility to be considered as a critical one. Some impressions have too many striations to indicate which stria is a driving edge or which one a trailing edge although they are very important marks for identification. In 3D perspective view, however, roughness of the surface is perceived intuitively and easily found both edges.

Next, we used another firearm (a 7.65 mm Browning auto model 1910). Width of impressions by this firearm are about 0.7 mm and narrower than the first firearm. Therefore, measuring roughness is considered more difficult for the device. Despite this difficulty, roughness of the surface is measured precisely. Then two different surfaces, which are printed in the same origin, are displayed in a monitor (Fig. 6). Appearances of the striations are identified, especially at left bottom regions. Note that the two shapes are virtually illuminated under the identical lighting condition.

### 4.2. Shape difference

Before shape comparison, a result of alignment is shown in Fig. 7. Two impression marks are printed in the same landmark (that is, the two have the same origin). The lower



Fig. 5. A conventional photo (left upper) and a virtual landmark impression (right bottom). A virtual impression can be moved and light source position can be changed easily in PC monitor by dragging mouse.

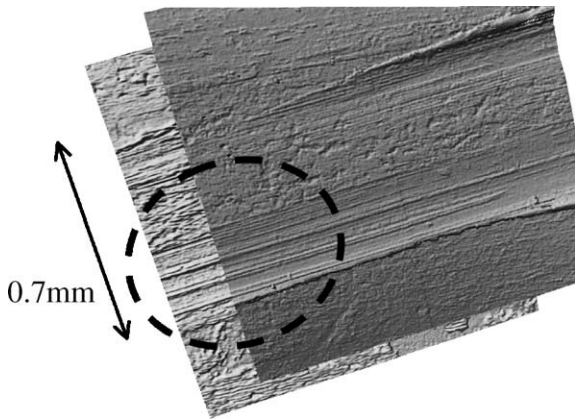


Fig. 6. An appearance-based comparison. Two virtual impressions are displayed simultaneously and striations in right bottom region coincide. Note that two surfaces are under the just same.

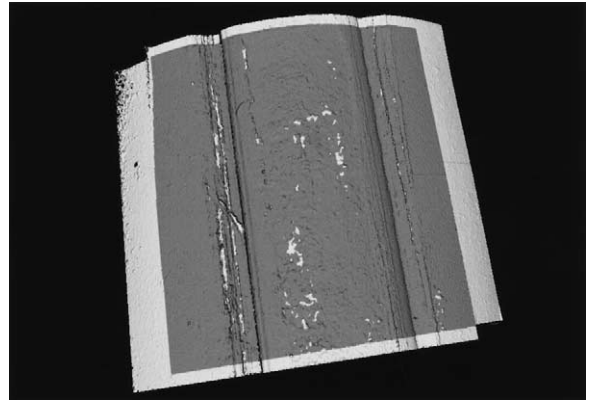


Fig. 8. Shape difference of two surfaces from the same firearm. The dark gray region indicates where the distance of two surfaces is less than threshold (0.015 mm). In other words, two shapes coincide in this region. Note that in almost whole overlapped region two shapes almost coincide.

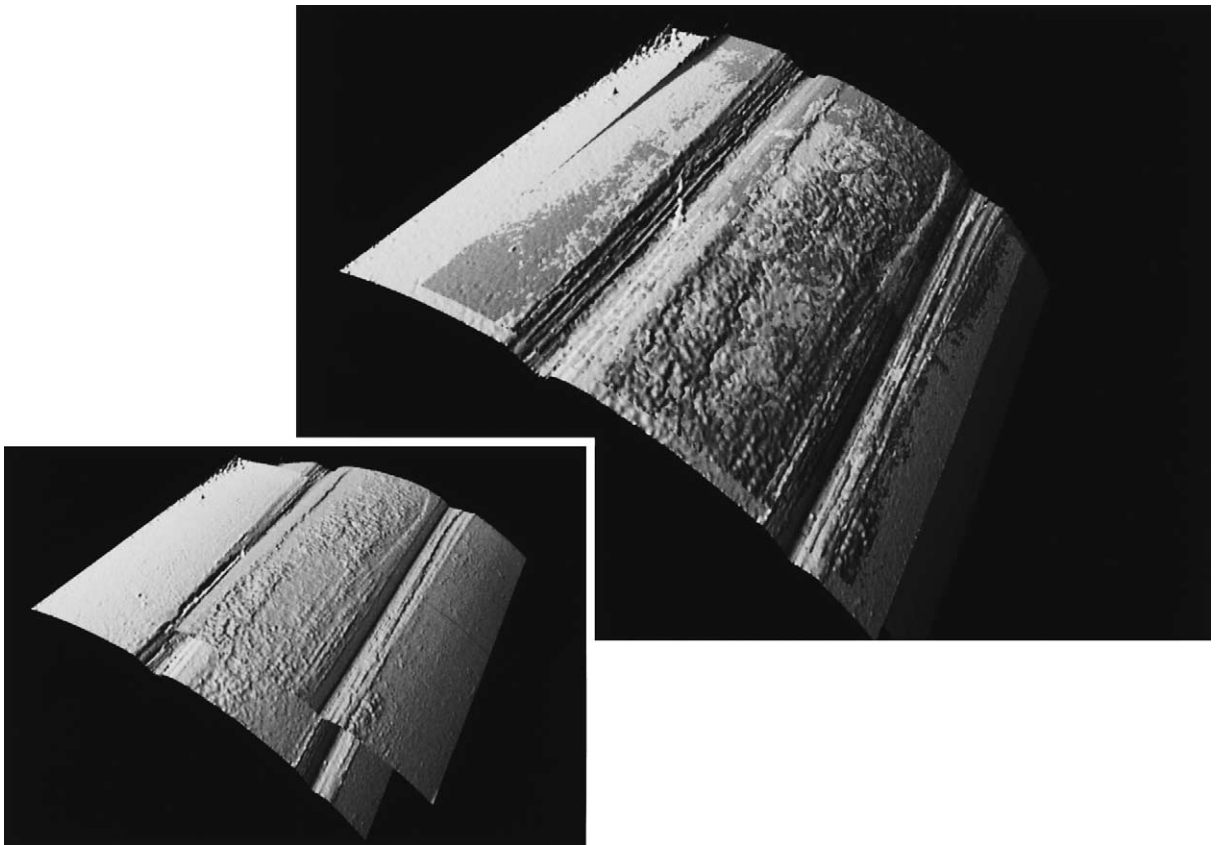


Fig. 7. An automatic alignment. The left bottom image shows initial condition and right top one shows the result. Two surface shapes are aligned automatically after several iterative calculations.



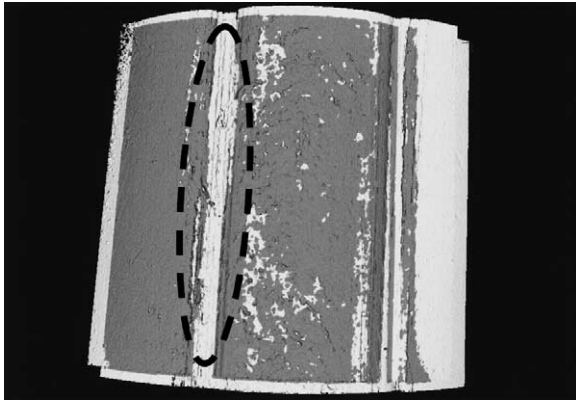


Fig. 9. Shape difference of two surfaces from different firearms. The light gray region, where the distance of two surfaces is over the threshold, is spread along the scratch direction, in spite of overlapped part.

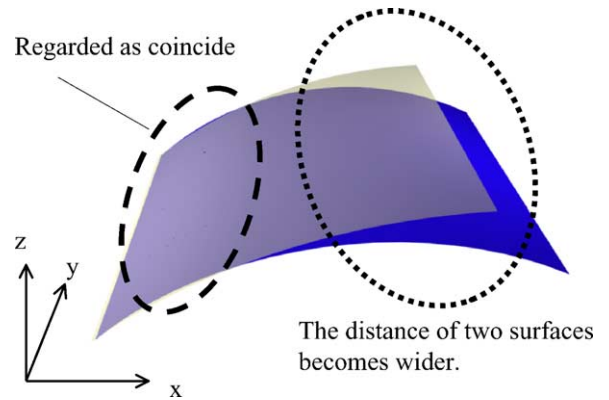


Fig. 10. Two smooth curved surfaces are modeled different landmark impressions. If two different shapes are aligned, the region of non-coincide is spread over along the scratch direction ( $y$ ).

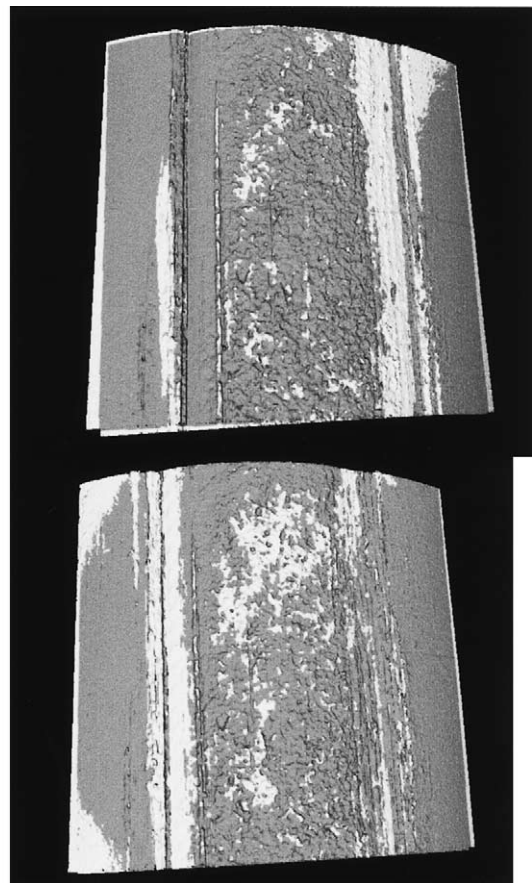
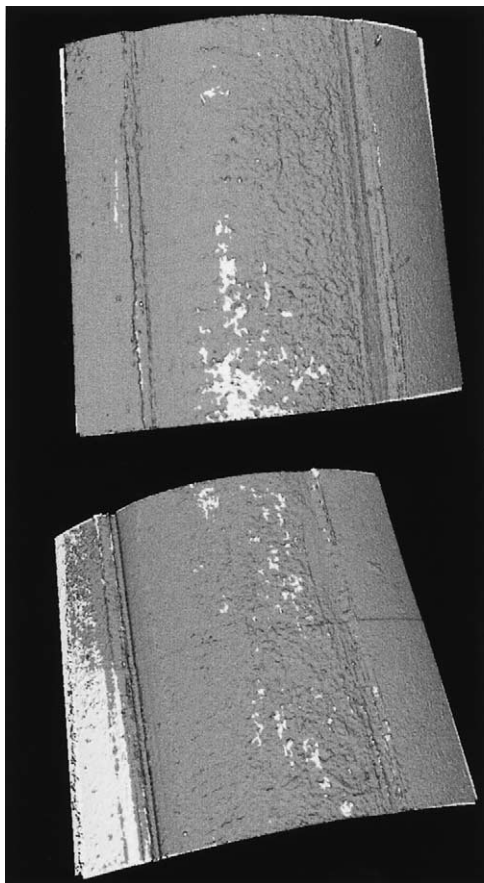


Fig. 11. Shape differences of four pairs of landmark impressions. The left side pairs are comparisons of impressions by the same landmarks while the right side pairs are those by different ones. Note that the non-coincide regions are spread over along the scratch direction in the right side pairs.

figure indicates original measurement data. Since each measurement data is described under each co-ordinate system, shapes of two surfaces don't coincide generally. After automatic alignment, two surface models are registered shown as the upper figure.

Fig. 8 shows the shape difference of the two surfaces after alignment. The shape difference is visualized according to the distances of corresponding pairs. If the distances are within a threshold (in this study, it is 0.015 mm), the area is displayed in dark gray region. While the distances are further than it, the area is colored light gray. In Fig. 8, almost all part of overlapped region is colored dark gray. It indicates that the two shapes are matched well.

On the other hand, a result, which compares two shapes in different origin, is shown in Fig. 9. Light dark region in Fig. 9 is wider than in Fig. 8. It indicates the number of corresponding pairs is fewer even in overlapped region. We can recognize intuitively that two shapes are different if they are fired from different firearms. In addition, the shape of non-coincide region spreads out along the direction of the scratch. This can be explained by following. Three dimensional shape of a landmark impression is considered almost

same along the scratch direction. Therefore, the shape along the width direction plays a significant role in shape identification. In this alignment method, two shapes are aligned in order to minimize the distance of them. Consequently, when comparing different shapes, surfaces at one side are close to while those at another side are far away. This is modeled as in Fig. 10.

Results of other comparisons are shown in Fig. 11. In these figures, the threshold is 0.015 mm. Two images in the left side are results of comparisons that compare two pairs from the same origins. We can find that the dark gray regions are spread almost all overlapped parts. This indicates these shapes coincide well. On the other hand, the right side images show two comparisons of two pair shapes in different origins. In these figures, non-coincide region is spread over along the scratch direction. As a result, we think that determining the threshold as 0.015 mm made clear visualization about matching regions.

It is very important to note that above comparing global curvature makes no sense if the bullet is deformed. A comparison of 3D topography on bullets is possible when they are not deformed.

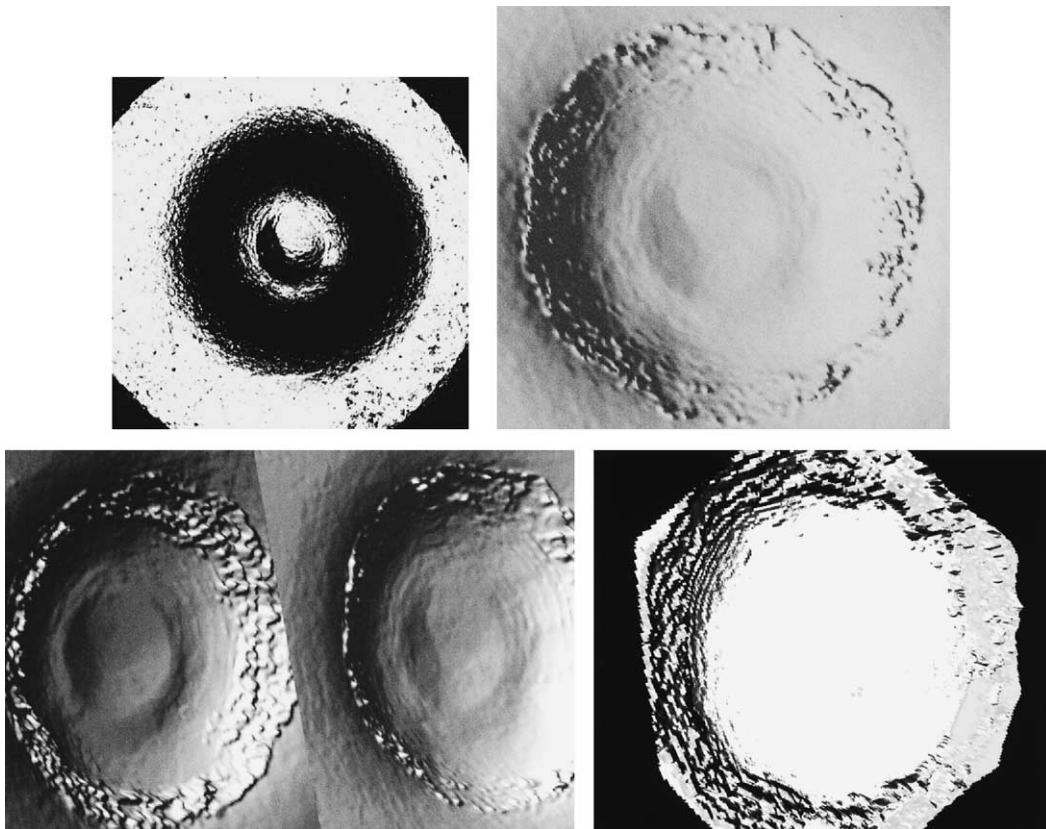


Fig. 12. A comparison of pin marks on cartridge bottom. The left top image is conventional photo. In this image it is hard to perceive the shape of the mark. The right top image is a virtual pin mark. The left bottom is two pin marks printed by the same firearm. The right bottom indicate shape difference of two marks. Almost whole shapes of hollow coincide.

## 5. Conclusions and future works

In this paper, we presented an algorithm for a shape comparison of impressions on bullets, by using 3D shape data. We measured surface topography by a confocal microscope and visualized virtual impressions on a PC monitor. Acquired 3D data were also utilized for numerical comparisons. After computing a “distance” between two surfaces for alignment, shape differences were visualized.

Our current goal is 3D visualization and comparison, not identification. To extend this method into bullet identification, we have to compare numerous pairs of bullets to determine the rigid threshold. This is one of the most important future works about this method.

We used striations on fired bullets mainly. It is not to say that this algorithm can be applied to other tool marks. We measured pin marks at the bottom of cartridges. The result of comparison is shown in Fig. 12. This indicates that this algorithm does well with other marks.

At present, we compared two shapes by global curvatures rather than elevations themselves. Since elevations on striations of bullets are very small, it is much difficult to measure and to compare these variations. Next we are going to

measure bigger tool marks and utilize elevations on surfaces for identification.

## References

- [1] J.D. Kinder, P. Prevot, M. Pirlot, B. Nys, Surface topology of bullet striations: an innovating technique, *AFTE J.* 30 (1998) 294–299.
- [2] J.D. Kinder, M. Bonfanti, Automated comparisons of bullet striations based on 3D topography, *For. Sci. Int.* 101 (1999) 85–93.
- [3] Z. Geradts, D. Zaal, H. Hardy, J. Lelieveld, I. Keereweer, J. Bijhold, Pilot investigation of automatic comparison of striation marks with structured light, *Proc. SPIE* 4243 (2001) 49–56.
- [4] T. Masuda, S. Imazu, T. Furuya, K. Kawakami, K. Ikeuchi, Shape difference visualization for old copper mirrors through 3D range images, in: *Proceedings of the Eighth International Conference on Virtual Systems and Multimedia*, 2002, pp. 942–951.
- [5] K. Nishino, K. Ikeuchi, Robust simultaneous registration of multiple range images, in: *Proceedings of the Fifth Asian Conference on Computer Vision*, vol. 2, 2002, pp. 454–461.
- [6] P.J. Besl, N.D. McKay, A method for registration of 3D shapes, *IEEE Trans. Pattern Anal. Mach. Intell.* 14 (1992) 239–256.